JOURNAL OF MATERIALS SCIENCE **38** (2003) 2571 – 2579

Suspension polymerization casting of lead zirconate titanate, part I: Acrylamide hydrogel system

W. MIAO*, J. W. HALLORAN
Department of Materials Science and Engineering, The University of Michigan, Ann Arbor, MI 48109, USA
E-mail: miaow@corning.com

D. E. BREI
Department of Mechanical Engineering and Applied Mechanics, The University of Michigan, Ann Arbor, MI 48109, USA

Suspension polymerization casting of lead zirconate titanate (PZT) filled acrylamide systems was studied. A high solid loading (51 vol%) PZT slurry with low viscosity (about 280 mPa·s at shear rate 10 s^{-1}) was obtained by optimizing the dispersant amount. The polymerization process for the monomer solution and PZT slurry were characterized with the help of the storage modulus measurement. For the monomer solution, the overall activation energy of gelation was calculated as 60–76 kJ/mol, while for the PZT slurry, this energy increased to 91 ± 9 kJ/mol. The drying, burnout and sintering processes were also addressed.

1. Introduction

Suspension polymerization casting (SPC) (or so-called gelcasting) is known as an effective way to build complex ceramic parts. Since SPC is a generic process, and is independent of the composition of the ceramic powder, it has been successfully applied to many ceramic systems [1–7]. In the current study, efforts are made to build complex piezoelectric devices via SPC.

In recent years, smart materials and structural design provide more flexibility to tailor the functionality of the device. Unfortunately, these designs are usually so complicated that special fabrication methods must be used to produce the desired structure. For instance, microfabrication co-extrusion methods were used to build micron size piezoelectric devices [8]. For macro size devices (typical feature size larger than 10 mm), SPC is a suitable way for fabrication, with the mold provided.

SPC process is much like general polymerization, except the former involves ceramic particles. In this process, the ceramic powder, solvent, dispersant, and binders are mixed to form a ceramic slurry. The binders are organic monomers instead of polymers or wax as in the case of injection molding. Before casting, the initiator is added to the slurry. After casting, the slurry is heated to gel, and form the desired shape in the mold. The cured green body is then removed from the mold, followed with a controlled drying step to remove the solvent in the body. At the final stage, the binder is burned out and the body is sintered to produce a dense part.

In the present study, SPC of lead zirconate titanate (PZT) is studied. This process can be divided into two categories according to the different kinds of solvents utilized: acrylamide hydrogel (solvent is water) and acrylate (solvent is organic or no solvent). The current study will be focused on the acrylamide system. In Part II, SPC process for acrylate systems will be addressed.

2. Experimental procedures

2.1. Processes

Table I lists all of the materials involved in the current study, including material composition, function, and sources. The starting material is PZT 586 powder (American Piezo Corp, Mackeyville, PA), with median particle size of 1.1 μm. The density of the powder is 7700 kg/m^3 and the specific surface area of this powder is 0.75 m^2/g. More than 60 different dispersants were tested and evaluated by sedimentation experiments. Among them, Emphos PS21A (aliphatic phosphate ester) (Witco Chemical, Dublin, OH) was proven to be the best dispersant for the PZT slurry. Therefore, it was used as the dispersant in the following study.

The composition of the slurry involves some organic monomers: single-functional N-(hydroxymethyl) acrylamide $H_2C{=}CHCONHCH_2OH$ (HMAM) (Aldrich, Milwaukee, WI) or methacrylamide $H_2C{=}C(CH_3)CONH_2$ (MAM) (Aldrich, Milwaukee, WI), difunctional N,N′-methylenebisacrylamide, $(H_2C{=}CHCONH)_2CH_2$ (MBAM) (Aldrich, Milwaukee, WI).

**Present address*: Weiguo Miao, Sullivan Park, DV-2, Corning Inc., Corning, NY14830, USA.

TABLE I Materials used in aqueous polymerization

Materials	Function	Compositions	Source
Lead Zirconate Titanate (PZT)	Ceramic powder	$Pb(Zr_{.52}Ti_{.48})O_3$	American Piezo, Mackeyville, PA
N-(hydroxymethyl) acrylamide (HMAM)	Monofunctional monomer	see (1)	Aldrich, Milwaukee, WI
N,N′-methylenebisacrylamide (MBAM)	Difunctional monomer	see (2)	Aldrich, Milwaukee, WI
Methacrylamide (MAM)	Monofunctional monomer	See (3)	Aldrich, Milwaukee, WI
Emphos PS21A	Dispersant	Aliphatic phsphate ester	Witco, Dublin, OH

(1) HMAM

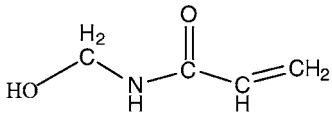

(2) MBAM

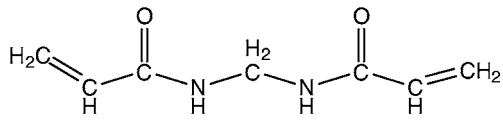

(3) MAM

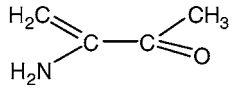

Since HMAM is toxic, the safer MAM was tested in order to substitute it for HMAM. These monomers were dissolved in deionized water to get a monomer solution. Ammonium persulfate, $(NH_4)_2S_2O_8$ (Aldrich, Milwaukee, WI) was selected to initialize the free-radical polymerization process. The typical compositions of the monomer solution and slurry are shown in Tables II and III respectively.

In the process, the dispersant was added to the monomer solution, then the PZT powder was added. If there is no notation, the solid load is 51 vol% and the dispersant level is 1 wt%. The mixed slurry was ball-milled for 48 h before casting.

The slurry was deaired in a rotary vacuum system until no air bubbles were observed. A diluted (25 wt%) aqueous solution of ammonium persulfate, was then added to the slurry. The slurry was then deaired for several minutes to ensure the air bubble-free and to provide for a homogeneous distribution of initiator.

TABLE II Typical composition of monomer solution

	Monofunctional HMAM[a] (or MAM[b])	Difunctional MBAM	Solvent water
wt%	14.4	1.2	84.4

[a]HMAM/MBAM monomer solution with viscosity 1.2 mPa·s, pH value 5.2.
[b]MAM/MBAM monomer solution with viscosity 1.5 mPa·s, pH value 8.1.

TABLE III Typical composition of PZT slurry

Chemicals	Composition
PZT586 Powder	51 vol% ($\rho = 7.7$ g/cm^3)
Monomer solution	49 vol% ($\rho = 1.01$ g/cm^3)
Dispersant	1 wt% of dried powder
Initiator ($(NH_4)_2S_2O_8$)	0.2 wt% of monomer solution

The mold in this study was made by cured epoxy, and was surface-coated with a mold release agent before casting. In the casting process, the slurry was slowly poured into the mold. A vacuum system was used for this operation to prevent air entrapping during pouring. The slurry-filled mold was then put into a drying oven at 60–90°C. Gelation time varied from several minutes to more than one hour, depending on the mold and the temperature. After gelation, the ceramic body was demolded (or partially demolded) and moved into a water-filled humidity chamber. The humidity was adjusted by changing the temperature of the chamber. Typically 75°C was selected as a temperature for humidity drying. The length of the humidity drying time depends on the thickness of the sample, usually only 2–3 h is needed for thicknesses less than 2 mm, while more than 10 h is needed for thicker parts.

After the ceramic body was partially dried, it was removed out of the humidity chamber and put in air for further drying. Afterwards, it was put into 85°C drying oven to remove the residual water. The drying time depends on the part size. It takes about 24 h to dry a 1 mm thick sample.

Since less than 3 wt% (of the dried powder) binder was used in the process, the burnout and sintering processes could be combined to simplify the process. The typical heating schedule is a ramp of 60°C/h to 900°C and then holds for 10 h, then a ramp of 120°C/h to 1275°C and soak for 4 h.

A typical SPC process flow chart is shown in Fig. 1.

2.2. Characterization

The rheological properties of the slurry were characterized by a rheometer with concentric cylinder C14

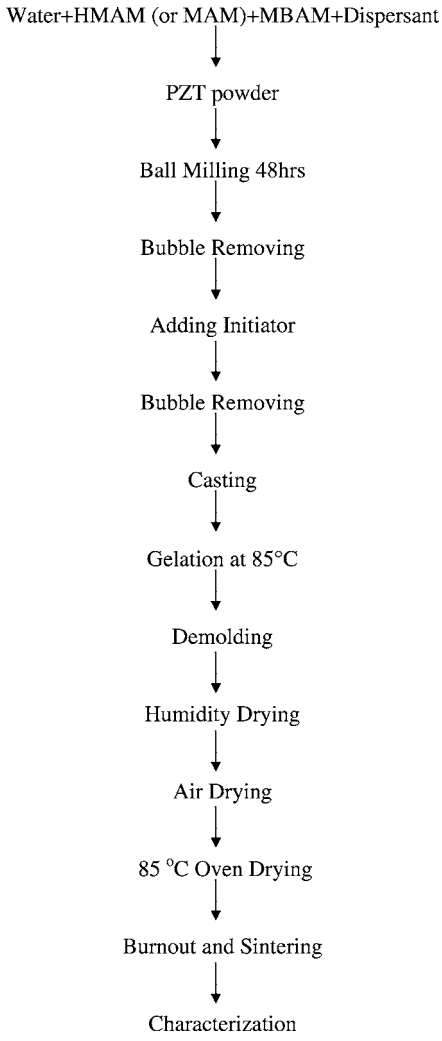

Figure 1 Aqueous SPC of PZT flow chart.

(Bohlin Rheolgi CS-50, Cranbury, NJ). The slurry was agitated for 5 min to reach equilibrium at room temperature. The rheological data were taken from the increasing shear rate curve. For each individual sample, three measurements were made to ensure the data were reproducible.

Oscillation measurements for the gelation process can be made using the same rheometer, with the C14 cup and bob (a special cover was used to minimize water loss). From these measurements, the complex viscosity μ^*, storage modulus G′, and loss modulus G″ were obtained. As a result, the gelation process can be partially characterized. For this measurement, the cup-bob gap was set to 0.5 mm, the frequency was set to 1 Hz, and the shear strain was set to 3×10^{-4}. Some influence on the gelation process, such as temperature, initiator amount, monomer type and ratio have been studied.

The pyrolysis behavior of the polymerized sample was characterized by the thermogravimetric analysis (TGA) using Cahn TG171 system (Cahn, Madison, WI). An air atmosphere was used and the heating rate was set as 10°C/min. The data were collected during the heating process. After reaching 600°C, the instrument was cooled down.

Scanning electron microscopy (SEM) was employed to observe the microstructure of the densified ceramics. In order to get detailed information about the microstructure, the PZT ceramics were polished and thermally etched. The densities of the sintered bodies were measured by Archimedes' method.

3. Results and discussion

3.1. Slurry behavior

The viscosity for the HMAM/MBAM monomer solutions is about 1.2 mPa·s. With the addition of PZT powder, the viscosity increases significantly to over 100 mPa·s. One of the principal requirements for SPC is to achieve high solids loading and a fluid slurry. The acceptable viscosity is about 300 mPa·s for SPC operation, with solids loadings about 50 vol%. To achieve this low viscosity, a dispersant is used to mitigate the van der Waals attraction force between the particles, thus decreasing the viscosity. In the present study, Emphos PS21A (pH = 1.6) was used to disperse PZT powder. Fig. 2 shows the experimental results in PZT slurries. When the dispersant is 0.4 wt%, the viscosity of the slurry is very high. A slight increase in dispersant to 0.5 wt% obtains a significantly lower viscosity; however, further increases in dispersant increases the viscosity. When the dispersant is more than 1.4 wt%, the viscosity is too high (over 500 mPa·s at 10 s^{-1}) and the slurry cannot be used for casting. Similar results on Al_2O_3 slurry were reported by Young *et al*. They found with a dispersant APA (ammonium polyacrylate) concentration of 7×10^{-6} L/g of powder, the Al_2O_3 particle surfaces were saturated with the dispersant. Assuming their powder has a specific surface area 8 m^2/g (manufacturer's data), the saturation concentration for the dispersant is 0.88 mg/m^2 of alumina powder surface. Further increases in amounts of APA did not decrease the viscosity of the slurry [9]. In the present study, 1 wt% dispersant was used to obtain a stabilized and fluid slurry, which equaled 13 mg/m^2 of PZT powder surface. This value is much higher than the case for the alumina slurry. One possible reason for this is that the PZT powder has a higher density than the alumina powder (7700 kg/m^3 vs. 3960 kg/m^3 respectively). With 1 wt% dispersant, the viscosity for 51 vol% loading slurry is about 280 mPa·s at a shear rate 10 s^{-1}. This low viscosity slurry is suitable for casting.

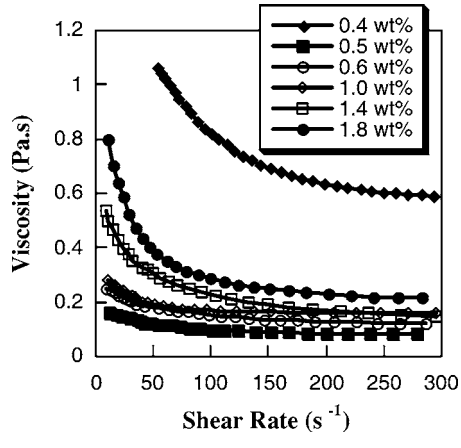

Figure 2 The effect of dispersant amount on the viscosity of the PZT slurry (HMAM/MBAM = 12 system). The solid load is 51 vol%.

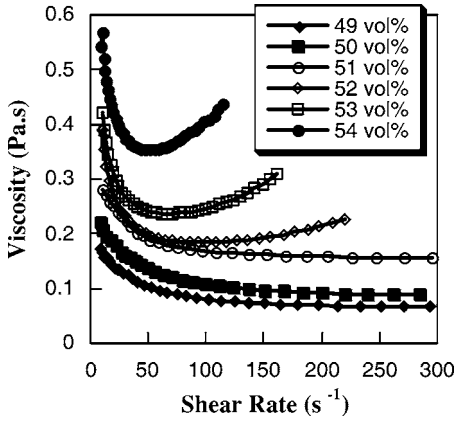

Figure 3 Solid load effect on the slurry behavior in HMAM/MBAM system, dispersant is 1 wt%. The mono- to di-functional monomer ratio is 12.

Fig. 3 shows the influence of solids loading on the viscosity behavior. For each of the solids loads, the slurry exhibits shear-thinning behavior in the low shear rate regime. The higher solid load slurries (>51 vol%) experience shear-thickening at shear rate over 50 s^{-1}, while at this regime, lower loading slurries have a plateau in the viscosity curve. Although 51 vol% and 52 vol% slurries have nearly the same viscosity behavior at intermediate shear rates, at low shear rates, the latter has a high viscosity that makes it undesirable for casting. As a result, with 1 wt% dispersant, 51 vol% is the maximum realistic loading for the PZT slurry in this study.

The above discussion is about slurries made with HMAM and MBAM. Since HMAM is very toxic, efforts were made to use the less toxic MAM [10]. While the viscosity for MAM/MBAM solutions (1.5 mPa·s) is almost the same as that for HMAM/MBAM solutions (1.2 mPa·s), replacing HMAM with MAM causes an increase in the slurry viscosity, as shown in Fig. 4. This increase may be due to pH changes in the system. The measured pH value for the HMAM/MBAM solution is 5.2, while that for MAM/MBAM is 8.1. With PZT powder and the dispersant, the pH values changed to 2.3 and 2.7 respectively, due to the acid nature of the dispersant. The pH value at the point of zero charge (pH_{pzc}) is about

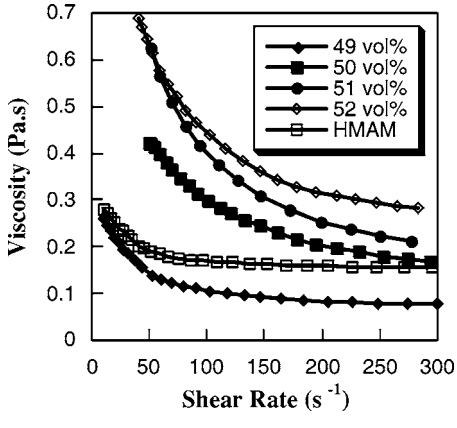

Figure 4 Solid load effect on MAM/MBAM system, dispersant is 1 wt%. HMAM/MBAM slurry with 51 vol% solid load is also shown in figure to compare the difference. The mono- to di-functional monomer ratio is 12.

10 to 11 for PZT [11]. Therefore, the PZT powder in the HMAM/MBAM solution may have more surface charges than that in MAM/MBAM system, resulting in a lower viscosity. Also, the slight viscosity difference in the monomer solutions may influence the behavior of the PZT slurry. As a result, to have a fluid slurry for polymerization, only 49 vol% solids loading can be used with the MAM/MBAM system. Low solids loading is a drawback for the MAM-based slurry. Fortunately, further investigation showed that this loading decrease did not significantly impact the sintering process. Therefore, it is possible to use MAM in replace of HMAM.

3.2. Monomer solution gelation process

During the gelation process, with polymerization continuing, the slurry becomes gradually thicker. By monitoring the change in the complex viscosity, the storage modulus G′ and loss modulus G″ of the gelation process can be partially delineated. In the present study, the storage modulus G′ was measured as a function of time, temperature, and gelation system. Most of the previous tests in the literature were performed at low temperatures, but since most of the polymerization processes are carried out at high temperatures (>50°C), the gelation behavior at high temperatures (over 50°C) can provide us more information on gelation start time. When testing hydrogel samples at high temperature, water loss is so significant that one cannot tell whether or not the modulus increase results from changes in the hydrogel structure [12]. Rueb and Zukoski used a preshearing process to get reliable data [13], but it is not applicable for this experiment. As a result, in the present work, the measurement data are used simply to calculate the reaction start time (or gel point). The gel point is the point where the storage modulus quickly starts to increase (in this case, $G' = 10$ Pa). It should be noted this definition is empirical, and the real gel point is difficult to determine, as will be discussed in Part II. At the gelation starting time, there is no infinite polymer cluster formed [14]. The mechanical properties are a good indicator of the gelation because they reflect the onset of gelation [14]. Further, in the following, we will see the measured data fit well with the theoretical data, which confirms our point.

A typical gelation process for the HMAM/MBAM monomer solution is shown in Fig. 5. Since copolymerization is one of the most important processes, in the following, we discuss only some common trends. The temperature effect is a prominent characteristic for the gelation process. As temperature increases, the initiator decomposes easily into free radicals and stimulates the polymerization process. This trend is clearly shown in the figure as the reaction starting time shortens, and the slope of the G′ curve increases as temperature increases. In application, a slightly higher temperature (85°C) was selected as the gelation temperature, because the epoxy mold used in the experiment has such a high heat capacity that much longer time is needed for gelation to take place at low temperatures (<85°C). Usually, 30 min are needed for gelation at 85°C, while more than 2 h at 60°C. For an epoxy tube mold, it takes

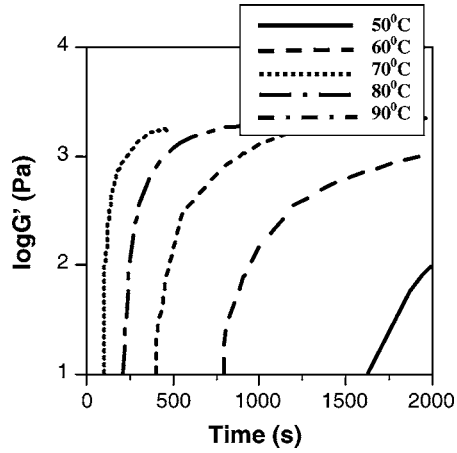

Figure 5 Typical gelation process for HMAM/MBAM monomer solution, with mono- to di-functional monomer ratio 12, and initiator amount 0.01 wt%.

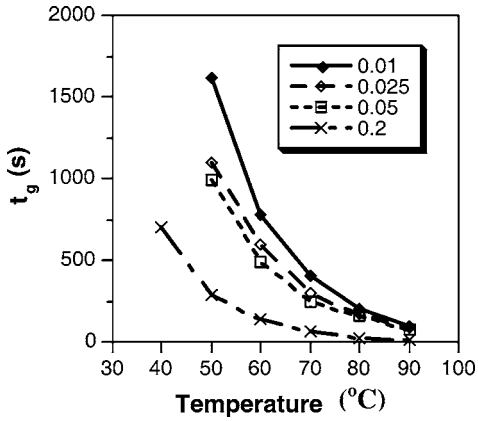

Figure 6 Initiator effect on the gelation time, for HMAM/MBAM monomer solution with mono- to di-functional monomer ratio 12, and different initiator amount 0.01%, 0.025%, 0.05% and 0.2%.

about 5 min for the outside mold to reach environmental temperature, and about 10 min for the mold interior to reach that temperature. As a result, a slightly longer gelation time is needed to build the PZT tubes.

Besides temperature effects, the initiator concentration has an impact on the polymerization process. Fig. 6 shows the relation between gelation time and different amounts of initiator in the monomer solution. It should be pointed out that in the experiment, 0.02 wt% initiator was used in the PZT slurry gelation, which equals about 0.2 wt% of the monomer in slurry. It is no surprise to see that increases in the initiator concentration lead to increases in process rates, especially in the low temperature regime. At 50°C, the gelation times for the monomer solutions with 0.01 to 0.2 wt% initiator are 1620 to 290 sec respectively. At 90°C, the initiator effect is not obvious, partially due to the fast reaction rates at the higher temperature. The effect of the initiator is due mainly to the change in the number of radicals in the system. At higher temperatures, this effect is not prominent because the reaction is very fast, and radicals are easy to diffuse to the unreacted area.

Gelation experiments were also done using different monomer ratios. Theoretically, with increases in concentration of the di-functional monomer, the strength of the gel should increase, which is the way

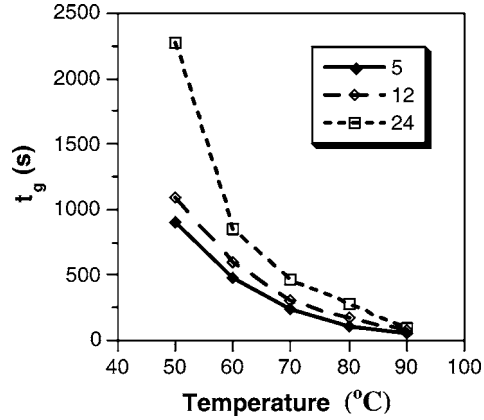

Figure 7 Mono- to di-functional monomer ratio effect on the gelation time. For HMAM/MBAM systems with monomer ratio 5, 12 and 24.

that the body strength can be manipulated [14–17]. Moreover, as shown in Fig. 7, with increases in the single-functionality monomer, the gelation time increases. This effect may be due to the reactivity and gel strength change in the system. The reactivity is described by the reaction rate: k_p. Although the k_p values for HMAM and MBAM are not available, the values for similar monomer acrylamide (AM) and n,n-dimethylacrylamide (DMAM) are 6000 and 27200 $(\text{mol}\cdot\text{s})^{-1}$ respectively [18]. Assuming that HMAM and MBAM have the same k_p values as that for AM and DMAM, it is reasonable to predict that MBAM will have a higher reactivity than HMAM. On the other hand, the gel strength alters with changes in the monomer ratios. With more single-functionality monomer present, the gel strength is weak and it takes more time for the storage modulus to reach the gelation criterion: 10 Pa. Therefore, both the contribution from reactivity and gel strength determines the short gelation time for more MBAM added to the system.

Because of safety considerations, efforts were made to substitute HMAM with MAM [10]. As shown in Fig. 8, the gelation process slows with the use of MAM as a single-functionality monomer. This is possibly due to change in the reactivity for the system. As shown for the MAM formula, there is a branch chain close to

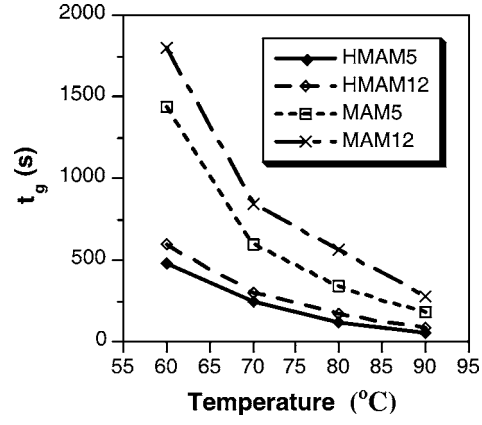

Figure 8 Monomer composition effects on the gelation time. For system with different single-functional monomer: HMAM or MAM, and with different mono- to di-functional monomer ratio: 5 or 12. Initiator amount is 0.025 wt%.

double bond; while for HMAM, it is a linear chain. The branch chain will slow down the reaction because of limited space to insert another chain. At 25°C in water, the reaction rate for MAM is only 800 $(\text{mol}\cdot\text{s})^{-1}$, much smaller than that for HMAM (which is similar to AM, about 18000 $(\text{mol}\cdot\text{s})^{-1}$) [18]. As a result, the gelation reaction slows for the MAM system.

3.3. PZT filled monomer solution gelation

Mechanical studies have been done to correlate the gelation processes with the mechanical property changes in slurry systems. Rueb and Zukoski [13] studied the elastic moduli of the slurry as a function of volume fraction and strength of interparticle attractions; Tokita *et al*. [19] investigated the critical behavior of the shear modulus of casein; Young *et al*. [9] reported the mechanical behavior of the aqueous gelcasting system; Morissette and Lewis [20] obtained information about the chemorheology of aqueous alumina-poly (vinyl alcohol) gelcasting suspensions. The above research shows the mechanical changes in the slurry can be a good indication for the gelation process. In the current study, with the addition of PZT powder, the slurry strength becomes higher, as compared with the monomer solution. Because of this effect, it should be noted that the measurement limit increases to around 10^2 Pa (under this value, the data are unstable). Moreover, around 10^2 Pa, the storage modulus for the slurry starts to increase very quickly. Therefore, we define the slurry gelation starting time as the time that the storage modulus reaches 10^2 Pa. Although this definition is different from the monomer solution case, it subsequently reflects the onset of gelation in all slurry systems.

Fig. 9 shows the typical modulus changes during gelation processes for the PZT slurry and monomer solution. With PZT powder, the gelation process will be retarded. It should be noted there are two stages in PZT slurry gelation. The detail about this two stage is complicated, and further study is needed to explain this.

The gelation times for different PZT slurries are shown in Fig. 10. It is no surprise to see the change in the monomer ratio does not impact the gelation process. As discussed above, the change in the monomer ratio impacts gel strength. But since gel strength is very

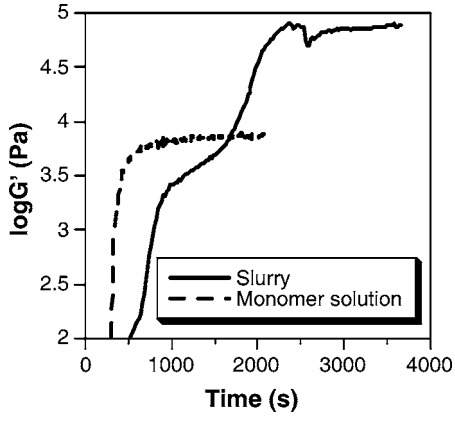

Figure 9 Gelation process for PZT slurry and monomer solution, with mono- to di-functional monomer ratio 12, and initiator of 0.2 wt% of monomer solution.

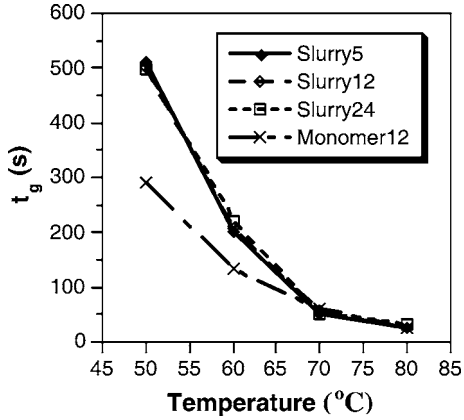

Figure 10 Gelation process for PZT slurries with different mono- to di-functional monomer ratio (5, 12, and 24), and monomer solution with mono- to di-functional monomer ratio 12. Initiator amount is 0.2 wt% of monomer solution.

weak, this effect is overshadowed by the addition of the PZT powder, because the slurry has a higher storage modulus than the monomer solution. Moreover, it seems that the gelation process is retarded with the addition of PZT powder. For instance, for the monomer solution, it takes about 280 sec for gelation to take place at 50°C; while for the PZT slurry, it takes about 500 sec. At 70°C and 80°C, this retardation effect is not obvious.

3.4. Overall activation energy

For free radical polymerization, the gelation time has an Arrhenius type relation with the overall activation energy: $t_g = A\exp(E_a/\text{RT})$, where t_g is the time gelation starts, A is a constant, and E_a is the overall activation energy. Both A and E_a values have an impact on the gelation time. This definition of the activation energy includes the effects of decomposition, propagation, and termination. Table IV lists the overall activation energy for different systems. For a monomer solution, the overall activation energies range from 60 to 76 kJ/mol. Taking into account experimental error, these results are in line with theoretical calculations (Appendix). Moreover, it should be pointed out that the overall activation energy does not vary dramatically with the change of

TABLE IV Composition effects on the overall activation energy

Composition	Overall activation energy (kJ/mol)*
HMAM12, with initiator 0.01 wt%	67 ± 7
HMAM12, with initiator 0.025 wt%	63 ± 6
HMAM12, with initiator 0.05 wt%	63 ± 6
HMAM12, with initiator 0.2 wt%	76 ± 8
HMAM5, with initiator 0.025 wt%	71 ± 7
HMAM24, with initiator 0.05 wt%	71 ± 7
MAM5, with initiator 0.025 wt%	68 ± 7
MAM12, with initiator 0.025 wt%	60 ± 6
Slurry with HMAM5, initiator 0.02 wt% of slurry	91 ± 9
Slurry with HMAM12, initiator 0.02 wt% of slurry	91 ± 9
Slurry with HMAM24, initiator 0.02 wt% of slurry	91 ± 9

*Uncertainty in E represents the largest data deviation from the values obtained by linear fit. The largest uncertainty was estimated as 10%, which used for all of the activation energies.

composition or the initiator amount. For instance, for the same monomer ratio, the change of the initiator amount does not change the activation energy significantly. The change of monomer from HMAM to MAM does not change the activation energy too much either. The retardation of MAM gelation is possible due to the small A value in the t_g formula. In the literature, for the AM (acrylamide)/MBAM system, a higher activation energy of 149.4 kJ/mol was reported by Young *et al.* [9] with catalyst, the activation energy would be lowered to 71.2 kJ/mol. In their experiment, the gel point was determined with the onset of temperature increase in the monomer solution. As shown in the Appendix, their definition of activation energy can be considered as the activation energy for decomposition, which is about 140 kJ/mol [21]. The calculation in the Appendix shows that by the definition of the gel point (the time at which G′ reaches 10 Pa), the theoretical overall activation energy should be approximately 76 kJ/mol, which matches well with the experimental data.

Compared with the monomer solution case, the activation energy for the PZT slurry shows a higher value, 91 ± 9 kJ/mol. This result indicates that the PZT powder may have a negative impact on the gelation. The effect of filler on gelation may be closely related with its physical and chemical impacts. From a physical point of view, the filler will block the transportation path and also act as a radical trap. Therefore, physically, the filler retards gelation. Chemically, the effect of the filler is a very complex chemical process, and both retardation and acceleration are possible. The overall result is a combination of these two effects. In the literature, most research shows the filler will have catalytic effect on the gelation [22–24]. On the other hand, there are several reports that the filler will have no or even a retardation effect on the gelation. For instance, Miranda *et al.* [25] found that filler retards gelation at high concentrations. Brady found that the addition of alumina had no influence on the photopolymerization rate [26]. For the current aqueous system, the addition of the PZT powder retards the gelation process. As a contrast, our result in the acrylate system shows the catalytic effect by the PZT powder. Therefore, the filler effect is closely related with the individual system.

3.5. Forming

The molds were made by stereolithography (SLA). The SLA detail was discussed elsewhere [27]. In this study, PZT thin tubes were made, since these tubes would be used as actuators. The wall thickness of the tubes is about 1.8 mm for the green body. The built parts are shown in Fig. 11. The lengths of the tubes vary from 40 to 150 mm. Because of the distinctive characteristic of polymerization process, the strength of the dried part is high enough to endure further polishing.

3.6. Drying, binder burnout and sintering

Drying is a key in the acrylamide SPC. The formed hydrogel exhibits a sharp volume contraction during drying. As the temperature increases, the gel loses a large fraction of its water. This results in a large volume contraction which may cause cracks in the green body. To prevent such problems, the drying process should be slow. In practice, a humidity chamber was used to restrict the drying process, and prevent cracking.

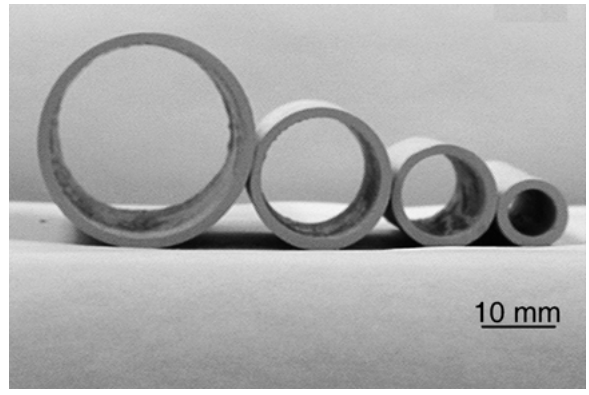

Figure 11 SPC tubes, with length vary from 40 to 60 mm, and thickness is about 1.8 mm.

One major merit for acrylamide SPC is a low binder content in the system. From the composition (Tables II and III), it is evident that the binder amount is less than 2 wt% in the slurry. Although in some cases, more binder is used to increase the part strength, the binder amount is still less than 3 wt%. Such low amounts of the binder will not cause any problems in the burnout process, as shown in Fig. 12. In this case, the binder amount is relatively high, but as the temperature increases to 500°C (ramp 1°C/min), no weight loss is observed. Therefore, aqueous SPC provides an inherent advantage in the burnout process.

Since the solid load in the slurry is 51 vol%, after the drying and burnout processing, the green body density is above 51 vol% (the drying shrinkage is 1.5–2 vol%). As a result, the sintering process for the SPC body is similar to that of a dry-pressed body. The polished surface of a sintered sample is shown in Fig. 13. Besides PZT grains, there are several defects present in the sample. Spot A is a pore caused by a PZT grain pulling out. Spot B is a hole originating from sintering. Spot C is dark grain enriched with Ni and Mg. The overall shrinkage for the PZT part is about 18% to 19%. The density is 7550 kg/m^3, which is about 98% of theoretical density, and denser than commercial PZT ceramics.

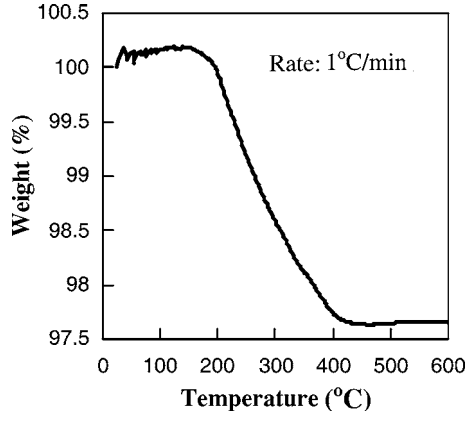

Figure 12 TGA test for SPC part. As can be seen, at temperature around 450°C, the binder has been removed.

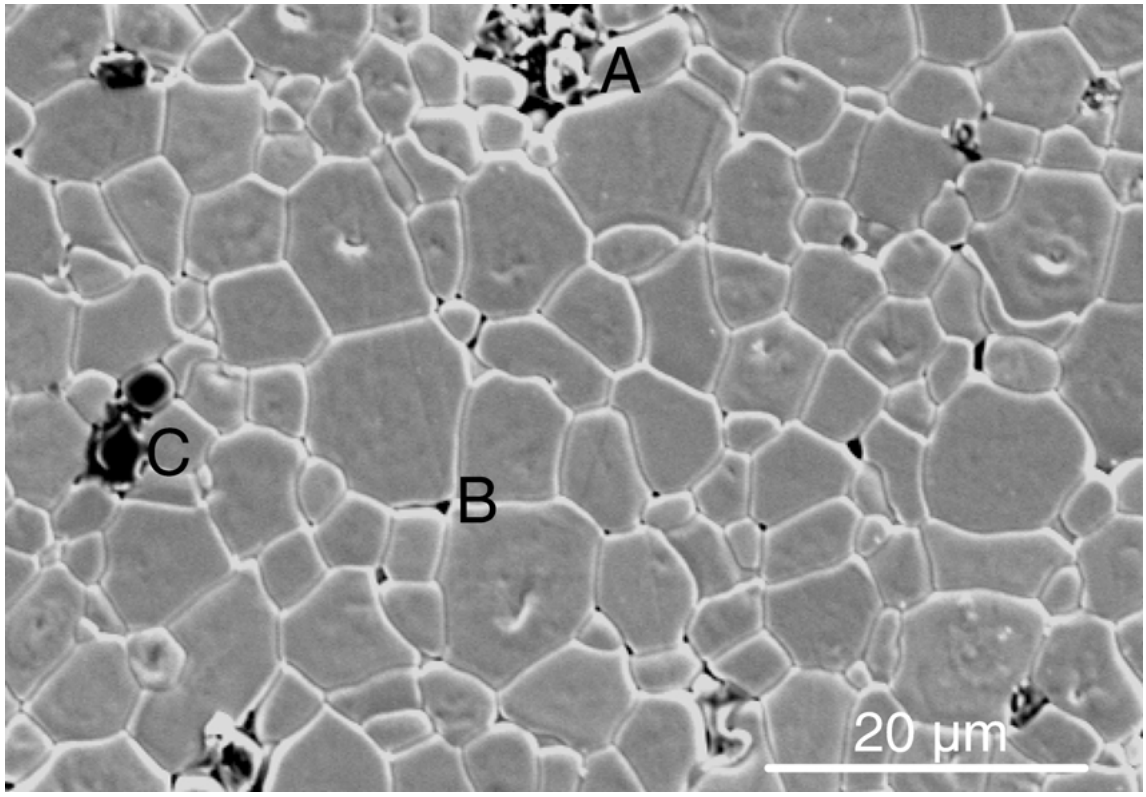

Figure 13 The polished surface of the sintered PZT ceramics. The big hole (A) is caused by pulling out of PZT grains during polishing. B is the small pore in PZT ceramics. Dark spot C is the grain rich with Ni and Mg.

3.7. Drawback of aqueous SPC

The biggest shortcoming for aqueous SPC is the lack of strength of the as-gelled green body. The gel strength can be adjusted by increasing the di-functional monomer content, but it is still not strong enough to build an internal connected ceramic parts. To build ceramic parts with an internal structure, high aspect ratio, and large surface area, a wax mold may be used for acrylamide system, or an acrylate system may be used, as discussed in Part II.

4. Conclusions

In the present study, SPC process for the PZT filled acrylamide (HMAM/MBAM and MAM/MBAM) systems was studied. A high solid loading PZT slurry with low viscosity was obtained by optimizing the dispersant and the amount of PZT powder. The gelation process for the monomer solution and PZT slurry were characterized by the storage modulus measurement. The overall activation energy for the monomer solution was calculated to be 60–76 kJ/mol, which matches well with the theoretical prediction. The addition of PZT powder retarded the gelation process, and the overall activation energy increased to 91 ± 9 kJ/mol. By using SPC technology, some PZT tubes were formed. The drying, burnout and sintering processes were also discussed.

Appendix

From the theory of polymerization [28], we have

$$\frac{1}{1-x}dx = \frac{K_p \cdot K_d^{1/2}}{K_t^{1/2}}(2fI)^{1/2}\,dt$$

where x is the monomer conversion, f the initiator efficiency, K_d, K_p and K_t are the initiator decomposition rate constant, reaction propagation rate constant and reaction termination rate constant, and I the initiator concentration.

$$\int_0^{x_0} \frac{1}{1-x}\,dx = \int_0^{t_0} \frac{K_p \cdot K_d^{1/2}}{K_t^{1/2}}(2fI)^{1/2}\,dt$$

Assume the temperature dependence of the rate constant may be written as:

$$K_t = A_t \exp\left(\frac{-E_t}{RT}\right) \quad K_p = A_p \exp\left(\frac{-E_p}{RT}\right)$$

$$K_d = A_d \exp\left(\frac{-E_d}{RT}\right)$$

Then, we get:

$$\ln(1-x_0) = A\left[\exp\left\{\frac{-\left(E_p - \frac{1}{2}E_t + \frac{1}{2}E_d\right)}{RT}\right\}\right]t_0$$

Since x_0 is constant (we defined $G' = 10$ Pa as starting point), rearrange the above formula,

$$t_0 = A' \exp\left(\frac{E_p - \frac{1}{2}E_t + \frac{1}{2}E_d}{RT}\right)$$

Therefore, we can see the idle time has a relation with the activation energy for three processes, if we define the overall activation energy $E_a = E_p - (1/2)E_t +$

$(1/2)E_d$, by using the published data, we can get the following estimation:

For acrylamide [28, 29]: $E_p = 11.7$, $E_t = 11.7$, $E_d = 138$, $E_a = 11.7 - 11.7/2 + 138/2 = 75$ kJ/mol;
For methacrylamide [28, 29]: $E_p = 15.5$, $E_t = 16.7$, $E_d = 138$, $E_a = 15.5 - 16.7/2 + 69 = 76$ kJ/mol.

Acknowledgements

This work is supported by DARPA (Grant # N00014-97-1-G009). The authors also want to thank Prof. Bike from Department of Chemical Engineering for help in chemorheology measurement.

References

1. K. VENKATASUAMY, R. WAACK, B. E. NOVICH and J. W. HALLORAN, U.S. Pat., 4978643 (1990).
2. G. A. BRADY and J. W. HALLORAN, *Rapid Prototyping Journal* **3** (1997) 61.
3. M. L. GRIFFITH and J. W. HALLORAN, *J. Am. Ceram. Soc.* **79** (1996) 2601.
4. *Idem., J. Appl. Phys.* **81** (1997) 2538.
5. M. L. GRIFFITH, "Stereolithography of Ceramics," Ph.D. thesis, The University of Michigan, 1995.
6. T.-M. CHU, J. W. HALLORAN and W. C. WAGNER, in "Case Studies in Ceramic Product Development," edited by A. Ghosh, R. E. Barks and B. Hiremath (American Ceramic Society, Westerville, OH, 1997) p. 119.
7. T.-M. CHU, "Solid Freeform Fabrication of Biomaterials," Ph.D. thesis, The University of Michigan, 1999.
8. A. T. CRUMM and J. W. HALLORAN, *J. Am. Ceram. Soc.* **81**(4) (1998) 1053.
9. C. YOUNG, O. O. OMATETE, M. A. JANNEY and P. A. MENCHHOFER, *ibid.* **74**(3) (1991) 612.
10. M. A. JANNEY, O. O. OMATETE, C. A. WALLS, S. D. NUNN, R. J. OGLE and G. WESTMORELAND, *ibid.* **81**(3) (1998) 581.
11. J. H. ADAIR, Pennsylvania State University, private communication.
12. K. S. ANSETH, C. N. BOWMAN and L. B. PEPPAS, *Biomaterials* **17** (1996) 1647.
13. C. J. RUEB and C. F. ZUKOSKI, *J. Rheol.* **41**(2) (1997) 197.
14. J. BASELGA, M. A. LLORENTE, I. H. FUENTES and I. F. PIEROLA, *Eur. Polym. J.* **25**(5) (1989) 471.
15. O. OKAY, H. J. NAGHASH and I. CAPEK *Polymer*, **36** (12) (1995) 2413.
16. H. KAWAGUCHI, Y. SUGI and Y. OHTSUKA, *J. Appl. Polym. Sci.* **26** (1981) 1649.
17. H. TOBITA and A. E. HAMIELEC, *Polymer* **31**(8) (1990) 1546.
18. J. BRANDRUP and E. H. IMMERGUT, "Polymer Handbook" (Wiley Inc., 1989) p. II-69.
19. M. TOKITA, R. NIKI and K. HIKICHI, *J. Chem. Phys.* **83**(5) (1985) 2583.
20. S. L. MORISSETTE and J. A. LEWIS, *J. Am. Ceram. Soc.* **82**(3) (1999) 521.
21. H. G. ELIAS, "Macromolecules: Synthesis, Materials and Technology" (Plenum Press, New York, 1983) p. 685.
22. J. Y. LEE, M. J. SHIM and S. W. KIM, *Mat. Chem. Phy.* **48** (1997) 36.
23. S. H. McGEE, *Polym. Eng. Sci.* **22**(8) (1982) 484.
24. S. G. KULICHIKHIN, A. Y. MALKIN, O. M. POLUSHKINA and V. G. KULICHIKHIN, *ibid.* **37**(8) (1997) 1331.
25. M. I. G. DE MIRANDA, C. TOMEDI, C. I. D. BICA and D. SAMIOS *Polymer*, **38**(5) (1997) 1017.
26. G. A. BRADY and J. W. HALLORAN, *J. Mater. Sci.* **33**(18) (1998) 4551.
27. P. F. JACOBS, "Rapid Prototyping & Manufacturing: Fundamentals of StereoLithography" (Society of Manufacturing Engineers, Dearborn, MI, 1992).
28. J. BRANDRUP and E. H. IMMERGUT, "Polymer Handbook" (Wiley Inc., 1989) p. II-335.
29. G. ODIAN, "Principles of Polymerization" (McGraw-Hill, 1970) p. 243.

Received 13 January
and accepted 26 March 2003